

# Parameter-Efficient Domain Adaptation of Physics-Informed Self-Attention based GNNs for AC Power Flow Prediction

Redwanul Karim<sup>1</sup>, Changhun Kim<sup>1</sup>, Timon Conrad<sup>2</sup>, Nora Gourmelon<sup>1</sup>, Julian Oelhaf<sup>1</sup>, David Riebesel<sup>2</sup>, Tomás Arias-Vergara<sup>1</sup>, Andreas Maier<sup>1</sup>, Johann Jäger<sup>2</sup>, Siming Bayer<sup>1</sup>

<sup>1</sup>Pattern Recognition Lab, Friedrich-Alexander-Universität Erlangen-Nürnberg, Erlangen, Germany

<sup>2</sup>Institute of Electrical Energy Systems, Friedrich-Alexander-Universität Erlangen-Nürnberg, Germany

**Abstract**—Accurate AC Power Flow (AC-PF) prediction under domain shift is critical when models trained on medium-voltage (MV) grids are deployed on high-voltage (HV) networks. Existing physics-informed graph neural solvers typically rely on full fine-tuning for cross-regime transfer, incurring high retraining cost and offering limited control over the stability-plasticity trade-off between target-domain adaptation and source-domain retention. We study parameter-efficient domain adaptation for physics-informed self-attention based Graph Neural Network (GNN), encouraging Kirchhoff-consistent behavior via a physics-based loss while restricting adaptation to low-rank updates. Specifically, we apply Low-Rank Adaptation (LoRA) to attention projections with selective unfreezing of the prediction head to regulate adaptation capacity. This design yields a controllable efficiency-accuracy trade-off for physics-constrained inverse estimation under voltage-regime shift. Across multiple grid topologies, the proposed LoRA+PHead adaptation recovers near-full fine-tuning accuracy with a target-domain RMSE gap of  $2.6 \times 10^{-4}$  while reducing the number of trainable parameters by 85.46%. The physics-based residual remains comparable to full fine-tuning; however, relative to Full FT, LoRA+PHead reduces MV source retention by 4.7 percentage points (17.9% vs. 22.6%) under domain shift, while still enabling parameter-efficient and physically consistent AC-PF estimation.

**Index Terms**—Graph Neural Networks, Physics-Informed Learning, Domain Adaptation, Low-Rank Adaptation, AC Power Flow

## I. INTRODUCTION

Accurate and fast solution of the AC power flow (AC-PF) equations underpins state estimation, contingency screening, and real-time security assessment in modern power systems [1]–[3]. Increasing renewable penetration, volatile operating points, and frequent topology changes primarily stress classical Newton–Raphson and fast-decoupled solvers in terms of computational throughput: while per-instance AC-PF solves remain reliable for updated  $\mathbf{Y}_{\text{bus}}$  and injections, repeated sparse Jacobian factorizations become a bottleneck in time-critical large-scale screening pipelines [4], [5]. Learning-based surrogates offer a complementary

path by incurring a one-time training cost and enabling fast per-scenario inference across many operating conditions.

GNN model the power grid as a graph and learn via neighborhood message passing along electrical connectivity, inducing a topology-aware and permutation-equivariant inductive bias that enables generalization across network sizes and topological configurations [6]–[8]. Message-passing GNN solvers and warm-start models—where neural predictors initialize iterative AC power flow or Optimal Power Flow (OPF) solvers to accelerate convergence—achieve strong performance for AC-PF and OPF [9]–[11], while GNN improve expressivity via attention-based aggregation [12]. However, purely data-driven GNN may violate Kirchhoff’s laws under distribution shift [13]. Physics-informed GNN embed the governing equations into the learning objective, improving extrapolation and physical feasibility [11], [14], but are typically trained and deployed in full precision, entailing higher computational and memory requirements.

From a deployment perspective, inference latency, memory footprint, and retraining cost are first-order constraints. Although quantization can reduce arithmetic cost and memory bandwidth [15], it is difficult to apply reliably to GNN due to degree-dependent aggregation and irregular dataflow [16]. We therefore focus on parameter-efficient fine-tuning as a practical means to reduce adaptation cost at deployment. At the same time, domain shift across grid regimes poses a central challenge: despite the topology-aware inductive bias of GNN, models trained on medium-voltage (MV) networks degrade when transferred to high-voltage (HV) systems due to changes in topology and operating statistics [7], [17]. Existing domain adaptation strategies typically rely on full fine-tuning, which is computationally expensive and induces substantial source-domain forgetting [18], [19], motivating approaches that explicitly control the stability–plasticity trade-off. Domain shift, physics-based regularization, and constrained adaptation capacity interact non-trivially, jointly shaping this stability–plasticity trade-off. Notably, explicitly augmenting edge features with detailed line parameters (e.g.,  $R/X$ ) to better capture cross-regime shifts would further increase feature dimensionality and model size, strengthening the case for parameter-efficient adaptation at deployment.

Corresponding author: redwanul.karim@fau.de. This work was conducted within the scope of the research project *GridAssist* and was supported through the “OptiNetD” funding initiative by the German Federal Ministry for Economic Affairs and Energy (BMWE) as part of the 8<sup>th</sup> Energy Research Programme. Source code and experimental configurations are available at <https://github.com/night-fury-me/efficient-graph-pf>.

**Relation to Prior GNN-Based Power-Flow Solvers.** Prior work establishes GNN as effective AC-PF surrogates [7], [9] and shows that physics-informed training improves physical consistency [13], [14], [20], [21]. However, cross-regime adaptation from MV to HV remains underexplored. This shift entails changes in voltage levels (partially normalized in p.u.), larger and different topologies, modified admittance matrices  $\mathbf{Y}_{\text{bus}}$ , and different line  $R/X$  ratios, which alter power-flow characteristics and reactive power demands. While GNNs encode connectivity, they do not inherently account for such parameter shifts. We study parameter-efficient adaptation of physics-informed GNNs for AC power flow under MV→HV regime shift. To the best of our knowledge, this is the first *systematic* analysis of low-rank adaptation in this setting, evaluating accuracy, physics-residual feasibility, optimization stability, and source-domain retention beyond the full fine-tuning baseline.

### Contributions.

- (i) We introduce low-rank adaptation of attention projections with selective prediction-head unfreezing for parameter-efficient transfer in physics-informed GNNs.
- (ii) We achieve near-full fine-tuning accuracy with  $> 85\%$  fewer trainable parameters while maintaining comparable physics residuals.
- (iii) We characterize the stability–plasticity trade-off via source-domain retention and few-shot target-domain scaling.
- (iv) We establish the efficiency–accuracy Pareto frontier for reliable cross-regime transfer under limited supervision.

**Paper Outline.** Section II presents the formulation, model, and adaptation strategies; Section III the datasets and setup; Section IV the cross-regime results and controlled architectural/adaptation studies; Section V concludes.

## II. METHODOLOGY

### A. Problem Formulation

We model a power grid as a graph  $\mathcal{G} = (\mathcal{V}, \mathcal{E})$ , where nodes  $i \in \mathcal{V}$  represent buses (PQ, PV, and slack) and edges  $(i, j) \in \mathcal{E}$  represent transmission lines. Each node is associated with input features  $\mathbf{x}_i \in \mathbb{R}^{d_x}$  encoding net active/reactive power injections, bus type indicators (PQ/PV/slack), and voltage setpoints for PV/slack; each edge with features  $\mathbf{e}_{ij} \in \mathbb{R}^{d_e}$  encoding line parameters (e.g.,  $R/X$ , susceptance). Let  $\mathbf{X} = \{\mathbf{x}_i\}_{i \in \mathcal{V}}$  and  $\mathbf{E} = \{\mathbf{e}_{ij}\}_{(i,j) \in \mathcal{E}}$  denote the collections of node and edge features.

The learning objective is to approximate the AC power-flow operator by a parametric predictor

$$f_\theta : (\mathcal{G}, \mathbf{X}, \mathbf{E}) \mapsto \hat{\mathbf{Y}}, \quad \hat{\mathbf{Y}} = \{(\hat{V}_i, \hat{\theta}_i)\}_{i \in \mathcal{V}}, \quad (1)$$

where  $(\hat{V}_i, \hat{\theta}_i)$  denote predicted voltage magnitudes and phase angles for all buses, with the slack complex voltage is fixed to their setpoints when computing loss and evaluation metrics.

Given training samples  $(\mathcal{G}^{(k)}, \mathbf{X}^{(k)}, \mathbf{E}^{(k)}, \mathbf{Y}^{(k)}) \sim \mathcal{D}_s$ , we train  $f_\theta$  on the source domain by minimizing the combined data-fitting and physics-informed objective:

$$\theta_s = \arg \min_{\theta \in \Theta} \mathbb{E}_{(\mathcal{G}, \mathbf{X}, \mathbf{E}, \mathbf{Y}) \sim \mathcal{D}_s} [\mathcal{L}_{\text{data}} + \lambda_{\text{PF}} \mathcal{L}_{\text{PF}}], \quad (2)$$

where the data-fitting loss  $\mathcal{L}_{\text{data}}$  is defined by the RMSE in Eq. (11) and the physics-informed residual loss  $\mathcal{L}_{\text{PF}}$  is given by Eq. (12). Here,  $\lambda_{\text{PF}} \geq 0$  is a scalar weighting coefficient that controls the trade-off between empirical data fidelity and adherence to Kirchhoff-consistent power-flow constraints, with larger values encourages stronger physical consistency at the potential cost of reduced data fit.

We consider a domain-adaptation setting with source and target distributions  $\mathcal{D}_s \neq \mathcal{D}_t$ , corresponding to different voltage regimes and operating statistics. Let  $\theta_s$  denote the source-trained parameters. The adapted parameters are obtained by restricting updates to a parameter-efficient adaptation subspace  $\mathcal{A}(\theta_s)$ :

$$\theta_t = \arg \min_{\theta \in \mathcal{A}(\theta_s)} \mathbb{E}_{(\mathcal{G}, \mathbf{X}, \mathbf{E}, \mathbf{Y}) \sim \mathcal{D}_t} [\mathcal{L}_{\text{data}} + \lambda_{\text{PF}} \mathcal{L}_{\text{PF}}], \quad (3)$$

where  $\mathcal{A}(\theta_s)$  denotes the parameter-efficient adaptation subspace (Sec. II-C), and  $\theta_s, \theta_t$  denote the source and adapted model parameters, respectively.

### B. Edge-Aware Self-Attention GNN

We employ a Transformer-style multi-head self-attention GNN with explicit edge-conditioned *attention biases*, following [14]. Let  $\mathbf{h}_i^{(\ell)} \in \mathbb{R}^{d \times 1}$  denote the column-vector embedding of node  $i$  at layer  $\ell$ , and let  $\mathcal{N}(i)$  be its one-hop neighbors. For head  $m = 1, \dots, M$  with per-head dimensionality  $d_h$ , we compute

$$\mathbf{q}_i^m = \mathbf{W}_Q^m \mathbf{h}_i^{(\ell)}, \quad \mathbf{k}_j^m = \mathbf{W}_K^m \mathbf{h}_j^{(\ell)}, \quad \mathbf{v}_j^m = \mathbf{W}_V^m \mathbf{h}_j^{(\ell)}, \quad (4)$$

where  $\mathbf{W}_Q^m, \mathbf{W}_K^m, \mathbf{W}_V^m \in \mathbb{R}^{d_h \times d}$ . Line features  $\ell_{ij} \in \mathbb{R}^{d_e \times 1}$  (e.g., admittance parameters) are mapped to a scalar, head-specific edge bias

$$\beta_{ij}^m = f_{\text{edge}}^m(\ell_{ij}), \quad f_{\text{edge}}^m : \mathbb{R}^{d_e \times 1} \rightarrow \mathbb{R}, \quad (5)$$

which augments the scaled dot-product attention logit:

$$s_{ij}^m = \frac{(\mathbf{q}_i^m)^\top \mathbf{k}_j^m}{\sqrt{d_h}} + \beta_{ij}^m, \quad \alpha_{ij}^m = \frac{\exp(s_{ij}^m)}{\sum_{k \in \mathcal{N}(i)} \exp(s_{ik}^m)}. \quad (6)$$

The head-wise aggregation is

$$\mathbf{h}_i^m = \sum_{j \in \mathcal{N}(i)} \alpha_{ij}^m \mathbf{v}_j^m, \quad \mathbf{h}_i^m \in \mathbb{R}^{d_h \times 1}, \quad (7)$$

and concatenation over heads followed by a linear projection yields  $\mathbf{h}_i^{\ell+1} \in \mathbb{R}^{d \times 1}$ . Injecting admittance-derived features as edge-dependent biases yields a directional, state-dependent propagation operator (generally  $\alpha_{ij}^m \neq \alpha_{ji}^m$ ) that better captures anisotropic electrical couplings and improves robustness under voltage-regime shifts and topology changes.

---

**Algorithm 1:** Parameter-Efficient Domain Adaptation of Physics-Informed Self-Attention based GNN

---

**Input** : Source dataset  $\mathcal{D}_s$ ; Target dataset  $\mathcal{D}_t$ ; GNN model  $f_\phi$ ; Physics weights  $\lambda_P, \lambda_Q$ ; LoRA rank  $r$

**Output** : Adapted model  $\hat{f}_\phi$

**Initialize:** Initialize base parameters  $\phi$ ; Initialize LoRA matrices  $\mathbf{A}_\ell \sim \mathcal{N}(0, \sigma^2)$ ,  $\mathbf{B}_\ell \leftarrow \mathbf{0}$

- 1 **foreach** *batch* from  $\mathcal{D}_s$  **do**
- 2     Predict  $(\hat{\mathbf{V}}, \hat{\theta})$ ;
- 3     Compute composite loss  $\mathcal{L}$ ;
- 4     Update  $\phi$  via gradient descent;
- 5 Freeze base parameters  $\phi$ ;
- 6 **foreach** *batch* from  $\mathcal{D}_t$  **do**
- 7     Apply low-rank updates  $\mathbf{W}'_\ell \leftarrow \mathbf{W}_\ell + \mathbf{A}_\ell \mathbf{B}_\ell$ ;
- 8     Predict outputs and compute  $\mathcal{L}$ ;
- 9     Update only  $\{\mathbf{A}_\ell, \mathbf{B}_\ell\}$  and the prediction head;
- 10 **return**  $\hat{f}_\phi$

---

### C. Parameter-Efficient Domain Adaptation

To enable controlled *model adaptation capacity* under domain shift, we restrict target-domain updates to low-rank perturbations of selected attention projection matrices, as summarized in Alg. 1. Specifically, we apply low-rank adaptation to the query, key, and value projections ( $\mathbf{W}_Q, \mathbf{W}_K, \mathbf{W}_V$ ). For any adapted projection  $\mathbf{W} \in \mathbb{R}^{d_{\text{out}} \times d_{\text{in}}}$ , we reparameterize

$$\mathbf{W}' = \mathbf{W} + \Delta \mathbf{W}, \quad \Delta \mathbf{W} = \frac{\alpha}{r} \mathbf{A} \mathbf{B}, \quad (8)$$

with  $\mathbf{A} \in \mathbb{R}^{d_{\text{out}} \times r}$ ,  $\mathbf{B} \in \mathbb{R}^{r \times d_{\text{in}}}$ , and  $r \ll \min(d_{\text{in}}, d_{\text{out}})$ , following [22]. We use rank  $r = r_{\text{loRa}}$  and scaling  $\alpha = \alpha_{\text{loRa}}$  in all experiments. All base parameters are frozen and only  $\{\mathbf{A}, \mathbf{B}\}$  are optimized. We additionally unfreeze the prediction head to regulate output-layer adaptation while preserving the learned message-passing backbone, explicitly controlling the stability–plasticity trade-off under domain shift.

### D. Computational Complexity

Let  $N = |\mathcal{V}|$ ,  $E = |\mathcal{E}|$ ,  $d$  denote the hidden dimension, and  $H$  the number of attention heads with per-head dimension  $d_h = d/H$ . For an edge-aware multi-head self-attention layer, the dominant costs stem from linear projections and edge-wise attention, giving

$$\mathcal{O}(Nd^2 + Ed), \quad (9)$$

with the dependence on  $H$  absorbed for fixed total hidden dimension  $d$ . With parameter-efficient adaptation, each projection is modified as  $\mathbf{W} + \mathbf{A} \mathbf{B}$  with rank  $r \ll d$ , incurring an additional cost

$$\mathcal{O}(Nrd), \quad (10)$$

which is lower order than the base  $\mathcal{O}(Nd^2)$  term and thus leaves the asymptotic complexity unchanged. In terms of parameters, full fine-tuning updates  $\mathcal{O}(d^2)$  weights per

projection, whereas LoRA reduces this to  $\mathcal{O}(r(d_{\text{in}} + d_{\text{out}}))$ , explaining the observed efficiency–accuracy trade-offs.

## III. DATASET AND EXPERIMENTAL SETUP

We synthesize physically plausible MV/HV datasets following Europe/Germany–typical overhead-line parameter ranges for series impedance and shunt charging (Table II) [23]–[25]. Each sample is a connected graph  $\mathcal{G} = (\mathcal{V}, \mathcal{E})$  with one slack bus and remaining PV/PQ buses; lines are modeled with  $\pi$ -equivalent circuits. MV grids emphasize higher  $R/X$  and shorter spans, whereas HV grids are reactance-dominated with longer spans.

Node features  $\mathbf{x}_i$  encode net injections ( $P_i^{\text{set}}, Q_i^{\text{set}}$ ), bus-type indicators, and voltage setpoints (for slack/PV buses); edge features  $\mathbf{e}_{ij}$  encode line physics via per-edge biases using admittance features. Initial states use  $|V_i^{(0)}| \in [0.9, 1.1]$  p.u. for slack/PV and  $|V_i^{(0)}| = 1.0$  p.u. for PQ buses with zero angle. Reference targets  $\mathbf{Y} = \{(V_i^*, \theta_i^*)\}_{i \in \mathcal{V}}$  are obtained by Newton–Raphson on the bus-admittance matrix  $Y_{\text{bus}}$  and setpoints  $\mathbf{S}^{\text{set}} = \{(P_i^{\text{set}}, Q_i^{\text{set}})\}$  under slack/PV/PQ constraints; non-convergent or disconnected cases are discarded.

All quantities are expressed in per-unit using  $(S_{\text{base}}, V_{\text{base}})$ . Data are split into train/validation/test with a fixed seed. We train a physics-informed GNN with edge-aware self-attention ( $d = 8$ ,  $d_{\text{hi}} = 32$ ,  $K = 40$ , 8 layers) using the combined RMSE loss (Eq. (11)) and physics residual loss (Eq. (12)) for 100 epochs (batch size 512) with AdamW (lr  $10^{-4}$ , weight decay  $10^{-3}$ ) and cosine annealing with warm restarts. We set  $r_{\text{loRa}} = 2$  and  $\alpha_{\text{loRa}} = 8$  unless stated otherwise. GPU acceleration is used when available.

## IV. RESULTS AND ANALYSIS

We evaluate MV→HV cross-regime adaptation under identical backbones and training budgets to test the central contribution that *parameter-efficient low-rank adaptation recovers near-full fine-tuning accuracy under domain shift while preserving physical consistency and enabling controllable stability–plasticity trade-offs*. Prediction accuracy is measured by

$$\mathcal{L}_{\text{data}}(\hat{\mathbf{y}}, \mathbf{y}) \triangleq \text{RMSE}(\hat{\mathbf{y}}, \mathbf{y}) = \sqrt{\frac{1}{N} \sum_{i=1}^N \|\hat{\mathbf{y}}_i - \mathbf{y}_i\|_2^2}, \quad (11)$$

reported for voltage magnitude and phase angle. Physical feasibility is quantified by the AC power-flow residual loss

$$\mathcal{L}_{\text{PF}} = \sum_{t=0}^{T-1} \gamma^{T-1-t} \left( \|\Delta P^{(t)}\|_2^2 + \|\Delta Q^{(t)}\|_2^2 \right), \quad (12)$$

with  $\Delta P^{(t)} = P^{\text{set}} - \Re\{V^t \odot (YV^t)^*\}$  and  $\Delta Q^{(t)} = Q^{\text{set}} - \Im\{V^t \odot (YV^t)^*\}$ , where  $V_k$  is the complex bus voltage,  $Y$  the admittance matrix, and  $\odot$  element-wise multiplication. Statistical significance is assessed using paired Wilcoxon signed-rank tests on  $N_{\text{wilcox}}$  stratified samples with Bonferroni correction (Table I) [26], [27]. We report both significance markers and effect sizes (e.g.,  $\Delta \text{RMSE}$ ,  $\Delta \mathcal{L}_{\text{PF}}$ ).

TABLE I: Cross-regime AC-PF prediction performance (MV→HV).

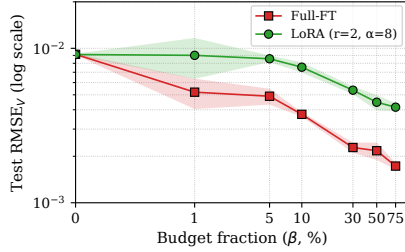
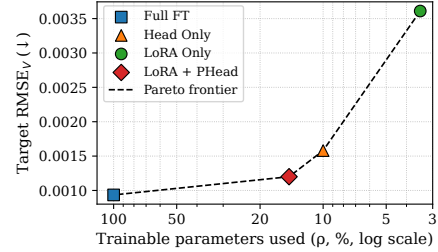
Method	Prediction Accuracy				Efficiency	
	RMSE <sub>all</sub> ↓	RMSE <sub>V</sub> ↓	RMSE <sub>θ</sub> (°) ↓	ℒ <sub>PF</sub> ↓	℘ <sub>reduced</sub> (%) ↑	ℛ <sub>ret</sub> (%) ↑
ZeroShot (Base)	$1.65 \times 10^{-2}$	$1.71 \times 10^{-3}$	$9.38 \times 10^{-1}$	2.57	—	—
<b>Full FT</b>	$9.35 \times 10^{-4}$	$3.61 \times 10^{-4}$	$4.95 \times 10^{-2}$	1.11	0%	22.6%
Head Only	$1.38 \times 10^{-3} \ddagger$	$4.19 \times 10^{-4} \ddagger$	$7.51 \times 10^{-2} \ddagger$	<b>1.11</b> ‡	88.50%	<b>22.3%</b>
LoRA Only	$3.61 \times 10^{-3}$	$1.05 \times 10^{-3}$	$1.98 \times 10^{-1}$	6.08	<b>96.56%</b>	17.3%
LoRA+PHead	<b><math>1.20 \times 10^{-3} \ddagger</math></b>	<b><math>3.53 \times 10^{-4} \ddagger</math></b>	<b><math>6.56 \times 10^{-2} \ddagger</math></b>	1.21 ‡	85.46%	17.9%

Best results are in **bold**. ↓ ↑ indicates lower/higher is better. RMSE: Root Mean Square Error. ℒ<sub>PF</sub>: Physics-informed PF loss. ℘<sub>reduced</sub>: Parameter reduction vs. Full FT. ℛ<sub>ret</sub>: MV retention, defined as  $\mathcal{R}_{\text{ret}} = 100 \cdot \text{RMSE}_{\text{MV}}^{\text{meth}} / \text{RMSE}_{\text{MV}}^{\text{base}}$ . ‡  $p < 0.01$  (paired Wilcoxon vs. Full FT over  $N_{\text{wilcox}} = 500$ ).

TABLE II: MV/HV parameter ranges.

Parameter (unit)	MV	HV
Base voltage (kV)	10	110
Base power (MVA)	10	100
Line length (km)	1–20	1–50
Series resistance (Ω/km)	0.5–0.6	0.15–0.20
Series reactance (Ω/km)	0.30–0.35	0.35–0.45
Shunt capacitance (nF/km)	8–14	8–10
Active power (MW)	[−5, 5]	[−300, 300]
Reactive power (MVAR)	[−2, 2]	[−150, 150]

MV/HV experimental setup: Each graph has 4–32 buses; datasets contain 90,030 (MV) and 45,030 (HV) samples; Train/Val/Test split 1:1:1


 (a) Few-shot target-domain adaptation vs. labeled fraction  $\beta$ .


(b) Efficiency–accuracy Pareto trade-off (RMSE vs. trainable parameters).

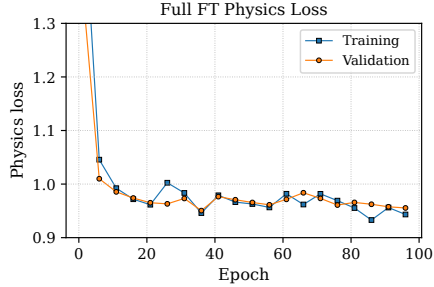
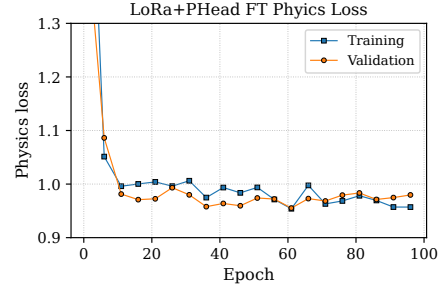

 (c) Physics-loss  $\mathcal{L}_{\text{PF}}$  during full fine-tuning.

 (d) Physics-loss  $\mathcal{L}_{\text{PF}}$  during LoRA+PHead adaptation.

Fig. 1: Cross-regime adaptation (MV→HV): few-shot scaling, efficiency–accuracy trade-off, and physics-loss dynamics for full fine-tuning and parameter-efficient adaptation.

### A. Cross-Regime Generalization Performance (MV→HV)

Zero-shot transfer yields  $\text{RMSE}_{\text{all}} = 1.65 \times 10^{-2}$ , indicating severe MV→HV domain shift, consistent with prior findings on regime sensitivity of learned power-flow surrogates [9], [10]. Full fine-tuning reduces error to  $9.35 \times 10^{-4}$ , establishing the adaptation upper bound.

LoRA+PHead achieves  $\text{RMSE}_{\text{all}} = 1.20 \times 10^{-3}$ , within  $2.6 \times 10^{-4}$  of Full FT while reducing trainable parameters by 85.46% (Table I), supporting **contribution (i)** [22]. Head-only under-adapts ( $1.38 \times 10^{-3}$ ), while LoRA-only degrades further ( $3.61 \times 10^{-3}$ ), indicating that attention-only low-rank updates cannot fully compensate regime-dependent rescaling, consistent with the role of attention projections in GAT message passing [12].

### B. Physical Consistency and Source-Domain Retention

Full FT achieves  $\mathcal{L}_{\text{PF}} = 1.11$ , while LoRA+PHead attains 1.21 (+9%,  $\Delta\mathcal{L}_{\text{PF}} = 0.10$ ), demonstrating that

parameter-efficient adaptation preserves physical feasibility at convergence, consistent with **contribution (ii)**. In contrast, LoRA-only incurs a large residual ( $\mathcal{L}_{\text{PF}} = 6.08$ ), indicating physically implausible solutions under insufficient adaptation capacity, in line with prior work on physics-informed regularization [13], [20], [21]. Training trajectories of  $\mathcal{L}_{\text{PF}}$  (Fig. 1c, Fig. 1d) show stable convergence for both Full FT and LoRA+PHead without divergence under heavily loaded regimes near voltage stability limits, indicating that restricting updates to low-rank subspaces does not degrade optimization stability for stiff AC power-flow losses [28].

Stability–plasticity is quantified by the source-retention score  $\mathcal{R}_{\text{ret}}$ , defined as source-domain RMSE relative to the zero-shot MV baseline (100% indicates no forgetting). LoRA+PHead balances strong target-domain adaptation with substantial source retention, whereas Head-only retains more but under-adapts, validating **contribution (iii)** [29].

### C. Few-Shot Adaptation and Sample Efficiency

We analyze performance as a function of labeled target fraction  $\beta$  (Fig. 1a). In the extreme low-shot regime ( $\beta \leq 5\%$ ), low-rank adaptation lags Full FT due to subspace-constrained bias under limited supervision [30]. For  $\beta \geq 10\%$ , LoRA+PHead approaches Full FT accuracy, characterizing the regime where parameter-efficient adaptation becomes Pareto-competitive (Fig. 1b) and supporting **contribution (iv)**.

### D. Efficiency–Accuracy Trade-off

The Pareto analysis (Fig. 1b) relates RMSE to trainable-parameter fraction  $\rho$ . Full FT ( $\rho = 1$ ) minimizes error at maximal cost; LoRA-only ( $\rho \approx 3.4\%$ ) underfits. LoRA+PHead ( $\rho \approx 14.5\%$ ) lies on the Pareto frontier, achieving near-Full-FT accuracy with a 6–7 $\times$  reduction in trainable parameters, reinforcing **contribution (i)** and **contribution (iv)**.

## V. CONCLUSION

We addressed cross-regime AC power-flow prediction under MV→HV domain shift using parameter-efficient adaptation of physics-informed self-attention based GNNs. By restricting updates to low-rank modifications of attention projections and selectively unfreezing the prediction head, the proposed approach encourages Kirchhoff consistency through a physics-informed loss while explicitly controlling adaptation capacity. Across multiple grid topologies, LoRA+PHead adaptation recovers near-full fine-tuning accuracy with an RMSE gap of  $2.6 \times 10^{-4}$  while reducing the number of trainable parameters by over 85%. Physical feasibility remains comparable to full fine-tuning, and LoRA+PHead exhibits a 4.7 percentage-point source-retention gap relative to Full FT under MV→HV domain shift. Together, these results demonstrate a practical efficiency–accuracy trade-off and controllable stability–plasticity for physics-constrained inverse estimation, enabling scalable deployment of learning-based AC power-flow solvers in evolving power systems.

## REFERENCES

- [1] B. Stott and O. Alsac, “Fast decoupled load flow,” *IEEE Transactions on Power Apparatus and Systems*, vol. PAS-93, no. 3, pp. 859–869, 1974.
- [2] A. A. El-Fergany, “Reviews on load flow methods in electric distribution networks,” *Archives of Computational Methods in Engineering*, vol. 32, pp. 1619–1633, 2025.
- [3] J. K. Skolfield and A. R. Escobedo, “Operations research in optimal power flow: A guide to recent and emerging methodologies and applications,” *European Journal of Operational Research*, vol. 300, no. 2, pp. 387–404, 2022.
- [4] W. F. Tinney and J. W. Walker, “Direct solutions of sparse network equations by optimally ordered triangular factorization,” *Proceedings of the IEEE*, vol. 55, no. 11, pp. 1801–1809, 1967.
- [5] E. A. Hailu, G. N. Nyakoe, and C. M. Muriithi, “Techniques of power system static security assessment and improvement: A literature survey,” *Heliyon*, vol. 9, no. 3, p. e14524, 2023.
- [6] F. Diehl, “Warm-starting AC optimal power flow with graph neural networks,” in *NeurIPS Workshop on Tackling Climate Change with Machine Learning*, 2019.
- [7] R. Ringsquandl, K. Kathan, and H.-A. Jacobsen, “Deep learning on power grids: Inductive learning on graphs,” *IEEE Transactions on Power Systems*, vol. 36, no. 5, pp. 4379–4388, 2021.

- [8] A. Deihim, D. Apostolopoulou, and E. Alonso, “Initial estimate of AC optimal power flow with graph neural networks,” *Electric Power Systems Research*, vol. 234, p. 110782, 2024.
- [9] B. Donon, R. Clément, B. Donnot, A. Marot, I. Guyon, and M. Schoenauer, “Neural networks for power flow: Graph neural solver,” *Electric Power Systems Research*, vol. 189, p. 106547, 2020.
- [10] N. Lin, S. Orfanoudakis, N. O. Cardenas, J. S. Giraldo, and P. P. Vergara, “PowerFlowNet: Power flow approximation using message-passing graph neural networks,” *International Journal of Electrical Power & Energy Systems*, vol. 160, p. 110112, 2024.
- [11] T. B. López-García and J. A. Domínguez-Navarro, “Power flow analysis via typed graph neural networks,” *Engineering Applications of Artificial Intelligence*, vol. 117, p. 105567, 2023.
- [12] P. Veličković, G. Cucurull, A. Casanova, A. Romero, P. Liò, and Y. Bengio, “Graph attention networks,” in *Proceedings of the International Conference on Learning Representations (ICLR)*, 2018.
- [13] X. Hu, H. Hu, S. Verma, and Z.-L. Zhang, “Physics-guided deep neural networks for power flow analysis,” *IEEE Transactions on Power Systems*, vol. 36, no. 3, pp. 2082–2092, 2021.
- [14] C. Kim, T. Conrad, R. Karim, J. Oelhaf, D. Riebesel, T. Arias-Vergara, A. Maier, J. Jäger, and S. Bayer, “Physics-informed GNN for medium-high voltage AC power flow with edge-aware attention and line search correction operator,” 2025.
- [15] R. Banner, I. Hubara, E. Hoffer, and D. Soudry, “Scalable methods for 8-bit training of neural networks,” *Advances in Neural Information Processing Systems (NeurIPS)*, vol. 31, 2018.
- [16] A. Tailor, V. K. S. Chandra, and S. Rajan, “Degree-Quant: Quantization-aware training for graph neural networks,” in *Proceedings of the International Conference on Learning Representations (ICLR)*, 2020.
- [17] H. F. Hamann, T. Brunschweiler, B. Gjorgiev, L. S. A. Martins, A. Puech, A. Varbella, J. Weiss *et al.*, “Foundation models for the electric power grid,” *Joule*, vol. 8, no. 12, pp. 3245–3258, 2024.
- [18] Z. Wu, S. Pan, F. Chen, G. Long, C. Zhang, and S. Y. Philip, “A comprehensive survey on graph neural networks,” *IEEE Transactions on Neural Networks and Learning Systems*, vol. 32, no. 1, pp. 4–24, 2021.
- [19] B. Sun and K. Saenko, “Deep coral: Correlation alignment for deep domain adaptation,” in *Proceedings of the European Conference on Computer Vision (ECCV)*, 2016, pp. 443–450.
- [20] S. de Jongh, F. Gielnik, F. Müller, L. Schmit, M. Suriyah, and T. Leibfried, “Physics-informed geometric deep learning for inference tasks in power systems,” *Electric Power Systems Research*, vol. 211, p. 108362, 2022.
- [21] A. B. Jeddi and A. Shafieezadeh, “A physics-informed graph attention-based approach for power flow analysis,” in *Proceedings of the IEEE International Conference on Machine Learning and Applications (ICMLA)*, 2021, pp. 1634–1640.
- [22] E. J. Hu, Y. Shen, P. Wallis, Z. Allen-Zhu, Y. Li, S. Wang, and W. Chen, “Lora: Low-rank adaptation of large language models,” *International Conference on Learning Representations (ICLR)*, 2022.
- [23] B. R. Oswald, *Vorlesung Elektrische Energieversorgung: Vorlesungsskript*. Eigenverlag / Hochschule (nicht offiziell veröffentlicht), 2005, korrigierte Ausgabe.
- [24] Z. Kremens and T. Sobierajski, *Analiza systemów elektroenergetycznych (Analysis of Electro Energy Systems)*. Warsaw: Wydawnictwa Naukowo-Techniczne, 1996.
- [25] G. Theil, “Statische stabilität von stromnetzen - erfahrungen bei analyse realer systeme,” in *Alternativen für die Energiezukunft Europas*, 2012, pp. 1–10.
- [26] F. Wilcoxon, “Individual comparisons by ranking methods,” *Biometrics Bulletin*, vol. 1, no. 6, pp. 80–83, 1945.
- [27] J. Demšar, “Statistical comparisons of classifiers over multiple data sets,” *Journal of Machine Learning Research*, vol. 7, pp. 1–30, 2006.
- [28] A. R. Bergen and V. Vittal, *Power Systems Analysis*. Prentice Hall, 1999.
- [29] M. McCloskey and N. J. Cohen, “Catastrophic interference in connectionist networks: The sequential learning problem,” *Psychology of Learning and Motivation*, vol. 24, pp. 109–165, 1989.
- [30] S. Geman, E. Bienenstock, and R. Doursat, “Neural networks and the bias/variance dilemma,” *Neural Computation*, vol. 4, no. 1, pp. 1–58, 1992.